Materials Today Advances 18 (2023) 100357

Contents lists available at ScienceDirect

Materials Today Advances

journal homepage: www.journals.elsevier.com/materials-today-advances/

One-pot synthesis of compact DNA silica particles for gene delivery and extraordinary DNA preservation

A. Ramos-Valle [a], L. Marín-Caba [a], L. García Hevia [a, **], M.A. Correa-Duarte [b, **], M.L. Fanarraga [a, *]

[a] The Nanomedicine Group, Valdecilla Health Research Institute IDIVAL, University of Cantabria, Avda Herrera Oria s/n, 39011, Santander, Spain
[b] CINBIO, Universidade Vigo, 36310 Vigo, Spain, Southern Galicia Institute of Health Research (IISGS), and CIBERSAM, Vigo, 36310, Spain

ARTICLE INFO

Article history:
Received 8 December 2022
Received in revised form
12 February 2023
Accepted 16 February 2023
Available online xxx

Keywords:
Transfection
Silica
Gene transfer
Nanoparticle
Sequential-gene expression

ABSTRACT

Repairing genetic defects using exogenous DNA is a major challenge the science is currently facing. This requires the design of vectors that can effectively encapsulate, protect and target nucleic acids to specific cells safely and precisely. Here we have designed silica-based physiologically responsive particles to encapsulate, store, and transfer DNA. Unlike existing vectors (*e.g.,* viral or lipidic particles), these DNA@SiO_2 systems are very stable at room temperature. We also demonstrate how they protect the encapsulated DNA from exposure to different biological and physicochemical stresses, including DNase, denaturation temperatures (>100 °C), or reactive oxygen species (ROS). Remarkably, upon cellular uptake, these vectors dissolve safely unpacking the DNA and transfecting the cells.

The versatility of the design is such that it can encapsulate genes without gene/size restrictions, in single or multiple layers of silica, so different genes can be expressed sequentially. This allows the time-controlled transcription of several genes, mimicking viral gene expression cascades, or even "fine-tuning" gene expression in transfected cells on demand. In addition, the method is easily scalable, reproducible, and inexpensive, enabling large-scale production and batch-quality testing, all of which are important for the personalized therapeutics industry. The high stability of these DNA vectors allows for easy and low-cost transport from the point of production to virtually any destination, making them unique as gene delivery tools.

1. Introduction

Decades ago, visionary scientists hypothesized that some diseases would be curable by delivering a healthy copy of a defective gene into the target cells. Since then, gene-transfer methods have evolved considerably and many strategies have been developed to "fine-tune" gene expression. So far, gene therapy has produced clinical benefits in patients with neuromuscular diseases, blindness, hemophilia, immunodeficiencies, or cancer [1]. However, vector toxicity, nonspecificity, or instability are some critical questions for the clinical validation of *in vivo* gene transfer.

A few years ago, the first *ex vivo* genetic modification gene therapy was approved to treat an inherited disease. The strategy consisted of using a lentiviral vector that encoded an anti-CD19 chimeric antigen receptor on autologous T cells [2]. Yet, safety concerns and clinical trial results that fell short of expectations have hampered progress. Among the main obstacles encountered are limited stability, reproducibility, and scalability of the gene delivery vectors [3,4]. Currently, the majority of the clinical trials in phase-I use recombinant viruses as vectors for gene delivery [5]. The most extensively used are adenovirus, retrovirus, and lentivirus. However, vector-related side effects (including inflammatory responses), or vector-mediated activation by insertion of proto-oncogenes limit *in vivo* administration of viral gene therapies [6–8].

The latest chemical advances in the production of biomaterials have improved the delivery of nucleic acids to cells [9]. Among these, liposomes and lipid-based systems are the most promising strategies. They are customizable, easy to prepare, show no restrictions on the size of the genes to be transduced, and have low immunogenicity or toxicity [10,11]. However, most of these vectors are not sufficiently stable as they must be prepared *in situ* leading to

* Corresponding author.
** Corresponding author.
E-mail address: fanarrag@unican.es (M.L. Fanarraga).

https://doi.org/10.1016/j.mtadv.2023.100357

variable efficiency. Also, in contrast to viral vectors, liposomes are difficult to target *in vivo*, typically accumulating in the liver or spleen [12].

Alternative systems rely on DNA-carrier proteins as vectors. Among these, nuclear proteins such as histones, some structural proteins of DNA viruses, or engineered chimeric fusion proteins are being investigated to improve specific recognition of target cells and to trigger receptor-mediated endocytosis and subcellular targeting [13]. Other synthetic gene carrier systems include calcium carbonate nanostructures, polymeric particles (*e.g.,* micelles, nanogels, cationic polymers, dendrimers, polymersomes, etc.), inorganic particles (*e.g.,* magnetic, gold, quantum dots, silica), carbon nanomaterials (*e.g.,* carbon nanotubes, graphene, carbon dots, and fullerenes) [14–18], or exosome-based vectors [19–25]. Most of these are mainly used *in vitro* or preclinically with varying success rates, while some are in the process of being validated as therapies. Still, there are many manufacturing procedures, standardization, and regulatory hurdles to overcome in the grand challenge of developing efficient and effective gene delivery vectors [26].

Silica (SiO_2) particles are valuable carriers for drug or nucleic acid delivery [27]. Silicon is the closest element to carbon, and in fact, many carbon compounds have homologous counterparts to silicon. Colloidal silica is highly biocompatible [28] and is currently used as an additive in food production, the cosmetic and pharmaceutical industries, and many nanometric designs [29–33]. Silica nanomaterials display well-defined morphologies and structures with customizable particle and pore sizes, large specific surface area, high mechanical and thermal stability, low toxicity, and excellent biocompatibility. Silica particles also offer the possibility of surface functionalization with many different ligands that for example could be used to target the nanoparticle to specific cell types. Indeed, silica shells are often used to endow a variety of different nanomaterials with these properties [34–37].

Interestingly, while colloidal silica is stable in some solvents (such as ethanol or isopropanol), it is degraded in aqueous media [38] and gets faster dissolved at physiological conditions (saline solution, pH 7.4) into silicic acid molecules that, *in vivo*, are excreted through the urine in both mice and humans [39,40]. Colloidal silica particle dissolution has been reported *in vitro* upon exposure to phosphate buffer, culture media, or serum [28,41–43], and also in the cell cytoplasm [42,43]. Concomitantly, silicon is detected extracellularly, suggesting that this element can cross the cell membrane without causing toxicity, even in fragile cells such as neurons [28,43,44]. The higher stability of amorphous silica nanoparticles at physiologically acidic pH (pH 5–6) is, in fact, a crucial advantage over their poor stability at pH above 7, where they degrade into silicic acid $Si(OH)_4$ [39,41]. This endows them with resistance to the lysosomal pH 5–6 when they are captured by the endo-lysosomal route, thus protecting the genetic material inside them from degradation. However, when they escape from the membranes into the cytosol, silica dissolution is observed at the physiological pH (7.4) of the cytosol. All these properties make silica an invaluable molecular carrier system in nanomedicine.

As observed in Fig. 1, some studies have already used silica vectors to transfer DNA by binding nucleic acids on the surface of particles [31,45–51]. These systems have the disadvantage that they expose nucleic acids to environmental DNases and are therefore not safe systems, as they could cause irreversible mutations and DNA damage. Another possible alternative is to encapsulate DNA in the cavities of mesoporous silica particles, but most of the DNA of therapeutic interest is too large to fit in the mesopores [31]. In some of these models, these particles are additionally coated to protect the DNA and prevent spontaneous release [52].

In light of this background, we aimed to develop a stable and bioresponsive silica-based DNA transfer system that could be applied for therapeutical purposes. A DNA transfer vector that would meet requirements such as batch and scalable synthesis, and storage/transport stability until use. As DNA is quite stable in saline and alcoholic solutions, here we decided to evaluate the encapsulation/decapsulation and transduction efficiency of plasmid DNA (pDNA) by introducing it directly into the Stöber mixture ("one pot" synthesis method). Our work shows that the designed system shows great stability, resistance, transfection efficiency, and design versatility.

2. Materials and methods

2.1. DNA production and purification

The pDNA was produced in *E. coli* DH5α using standard procedures (Table S1). Bacteria were cultured overnight in Luria-Bertani (LB) broth medium. The DNA was extracted and purified using a kit (PureLink™ HiPurePlasmid Maxiprep, ThermoFisher) following the manufacturer's protocol. DNA was precipitated and resuspended in double distilled water (ddH_2O) free nucleases at 2.5 μg/mL for direct use in particle synthesis.

2.2. Plain SiO_2 particle synthesis

Plain monodispersed silica spheres were prepared by the Stöber modified method (Table S2) [35,53]. In a typical experiment, a mixture of ethanol (EtOH) and dH_2O was vortexed in a bench-top thermoshaker at 1200 r.p.m for 5 min. Next, ammonia (NH_3, 25%, aqueous solution, Suprapur®) and Tetraethoxysilane (TEOS, 99%, Sigma Aldrich) were added to the mixture that was vortexed for 2 h at 20 °C before DNA@SiO_2 particle precipitation. The particles were washed in several cycles of centrifugation/redispersion and were stored in EtOH.

2.3. DNA@SiO_2 particle synthesis and characterization

Silica beads containing pDNA were prepared by a modification of the Stöber method. In brief, the EtOH was mixed with 5 μg of the corresponding pDNA (0.14×10^{-4} M) dispersed in 18 μL of nuclease-free ddH_2O (10 M) and was stirred at 1200 rpm for 5 min (Tables S2–S3). 17.3 μL of NH_3 25% (1.22 M) and 5.6 μL TEOS (0.24 M) were next added to the reaction that was vortexed for 2 h. DNA@SiO_2 spheres were centrifuged, washed, and stored in EtOH. Dynamic Light Scattering (DLS) and zeta potential characterization of the particles were carried out on a Malvern Ultra Zetasizer at 25 °C in a PBS solution. Transmission electron microscopy (TEM) images were obtained with a JEM1011 microscope equipped with a high-resolution Gatan digital camera (JEOL, Japan). TEM measurements were performed in samples dispersed in ethanol and dried on carbon film-coated copper grids. A total of $n = 100$ particles in 3 replicas were measured for each sample. The data shown are the mean ± standard deviation (SD).

2.4. DNA extraction from the particles and electrophoretic analysis

DNA@SiO_2 particles were dissolved in phosphate-buffered saline media (PBS, pH 7.4) inside a 14 kDa cut-off cellulose dialysis membrane (Sigma) for 72 h. The released DNA was precipitated from the media with NaCl 0.2 M in ice for 1 h, centrifuged at 15,000 *g* for 30 min, and run a 1% agarose gel for electrophoresis. A total of 1 μg of DNA was loaded in the gel, stained with ethidium bromide, and observed in a UV transilluminator.

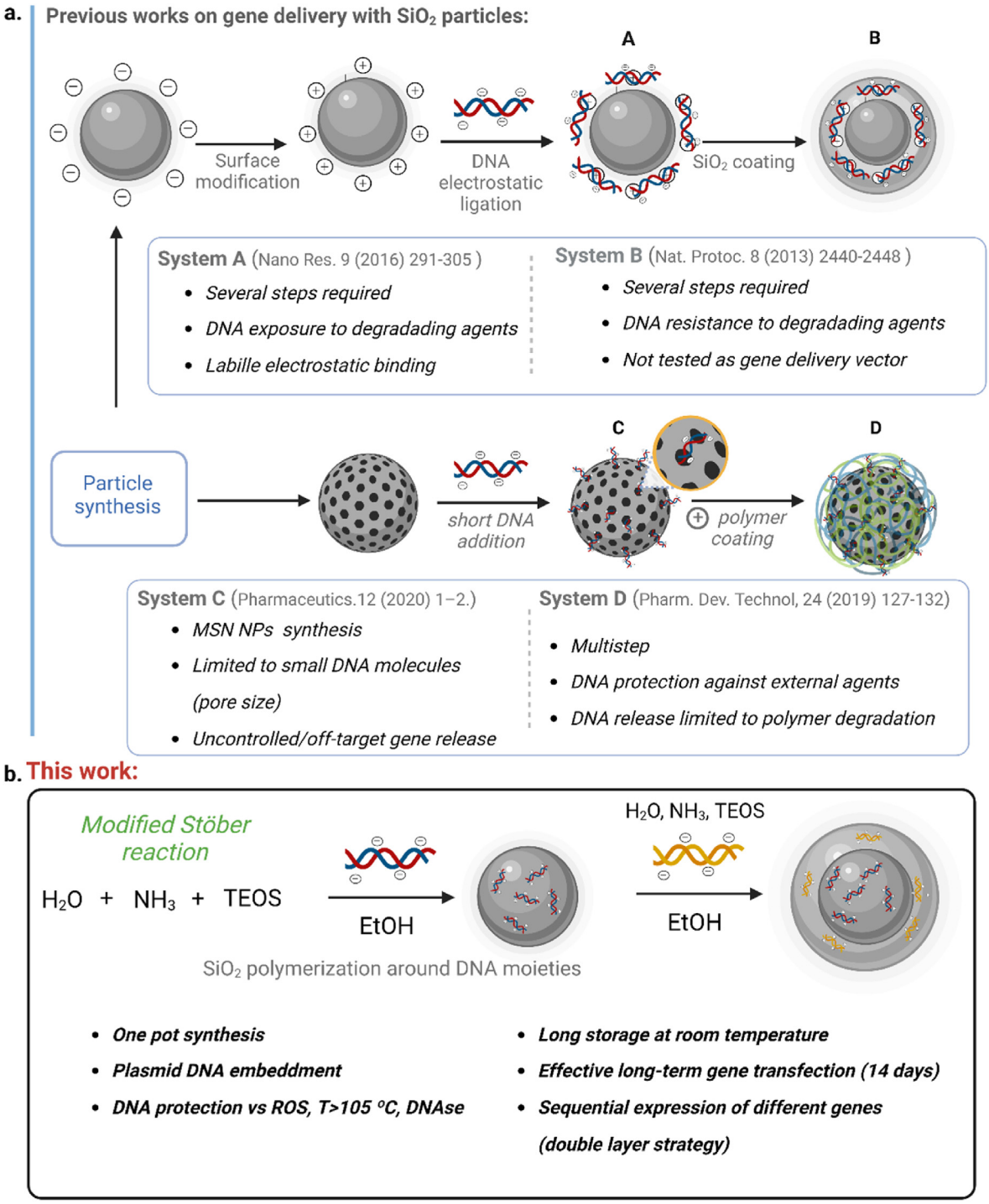

Fig. 1. General scheme of silica particles as gene delivery vectors a) Recent designs of non-viral vectors for gene delivery based on silica. Systems A-B are prepared by (i) bare amorphous SiO_2 particle synthesis (negative surface), (ii) surface modification with amines or cationic ligands to (iii) furtherly conjugate DNA molecules. In system B, DNA cargo is protected with SiO_2 extra-layering (iv). Systems C-D are based on mesoporous silica nanoparticles and require small DNA molecules to fit inside the pores. System D implements a cationic polymer coating on the surface to stabilize and protect the genetic cargo. b) The outline of the DNA@SiO_2 synthesis and main biological properties are described herein.

2.5. Cell culture, in cellulo DNA@SiO_2 particle dissolution, and viability assays

HEK 293T (human embryonic kidney) cells were maintained in Iscove's Modified Dulbecco's Medium (IMDM) supplemented with 10% fetal bovine serum and antibiotics. HeLa cells were maintained in Minimum Essential Medium (MEM) supplemented with 10% fetal bovine serum and antibiotics. Cultures were maintained in a 5% CO_2 incubator at 37 °C. HEK 293T and HeLa were seeded in a 6-well plate at a density of 5×10^5 per well and allowed to attach to the plate overnight. DNA@SiO_2 particles were resuspended in medium to a final concentration of 100 μg/mL and were added to the cells that were incubated for 16 h before media replacement (2 mL IMDM medium containing the particles per well). For

ultramicrotomy and TEM observation, cells were fixed with 3% glutaraldehyde in 0.12 M PBS for 24 h, were post-fixed in 2% buffered osmium tetroxide, dehydrated in a graded acetone series, and embedded in Araldite resin. Ultrathin sections of ca. 70 nm thick, were obtained on an LKB ultramicrotome, stained with lead citrate and uranyl acetate. TEM was a JEOL JEM 1011 operated at 120 kV. Cell viability was assessed in cultures treated with 100 μg particles/mL for 24 h (24-well plate, 50.000 cells/well seeded, 0.5 mL medium/well). Particle-treated cells were harvested, centrifuged, washed twice with PBS, and resuspended 50 μL of a solution of 0.1% of Trypan Blue for live/dead cell counting in a Neubauer chamber.

2.6. Transfection efficiency assays and flow cytometry

For transfection with DNA@SiO_2 particles, HEK 293T and HeLa cells were seeded in a 6-well plate at a density of 5×10^5 cells per well and were allowed to attach to the plate overnight. Cells were treated with a final concentration of 100 μg particles/mL in the media and were incubated for 16 h before media replacement (2 mL medium/well). As a control with standard reagents, HEK 293T cells were also transfected with Lipofectamine™ 2000 following the manufacturer's instructions. In brief, 3.13 μL of pDNA:Lipofectamine™ 2000 were combined with IMDM medium and 2.5 μg of pDNA. Cells were incubated with 100 μL of the mixture and 400 μL for 4 h, before media replacement. Finally, the cultures were washed twice with PBS and fixed in 4% PFA solution for 15 min for fixation before fluorescent microscopy observation or quantification by flow cytometric analysis. Cells were harvested at the indicated times and were centrifuged and washed twice with PBS and fixed in PFA/PBS 4% solution for 15 min. A total of *ca.* 10,000 cells were analyzed using a CytoFLEX (Beckman Coulter) equipped with excitation 3 lasers (488 nm × 50 mW; 638 nm × 50 mW; 405 nm × 80 mW) and 13 fluorescence detectors. Quantification of cells treated with HSP70:GFP@SiO_2@H2B:mCherry@SiO_2 particles was performed by spectral flow cytometric analysis. A minimum of *ca.* 10,000 cells were analyzed per experimental replica (a total of 3 replicas for each experimental group). Data are shown as the mean ± standard deviation (SD).

2.7. DNA@SiO_2 particle treatment with DNase, ROS, high temperature, UVC

The stability of YFP-DNA@SiO_2 particles was assessed under different extreme conditions; (i) 150 μg of the synthesized particles were treated with two ROS-producing solutions: H_2O_2 (12.5 μL, 20 mM $_{(aq)}$), $CuCl_2$ (17.5 μL, 500 μM) [54]; (ii) 150 μg of synthesized particles were heated to 105 °C for 45 min; (iii) 150 μg were exposed to direct UVC light 36 W for 60 min, or (iv) 1000 μg of DNA@SiO_2 (with 5 μg of pDNA encoding H2B:YFP protein) were treated with DNase type I (5 U) (Sigma-Aldrich) for 10 min at 37 °C (following commercial protocol 1U DNAse type I per μg of pDNA). The DNase reaction was quenched at 70 °C for 15 min to destroy the nuclease. After all these treatments, the DNA@SiO_2 particles were washed 2x with EtOH and MiliQ water. Treated particles were transfected in parallel using the as-prepared particles as controls for quantification. The experiment was done in triplicate.

2.8. Synthesis and characterization of double/triple-layered particles

DNA@SiO_2 particle nuclei (Fig. 5 #1, internal cores) were prepared as described. EtOH was mixed with 5 μg of the corresponding pDNA (0.14×10^{-4} M) dispersed in 31.3 μL of nuclease-free ddH_2O (14 M) and was stirred at 1200 rpm for 5 min 5.5 μL of NH_3 25% (0.34 M) and 5.6 μL TEOS (0.24 M) were next added to the reaction that was vortexed for 2 h. DNA@SiO_2 spheres were centrifuged, washed, and finally stored in EtOH. For the external silica layer (Fig. 5, #2), 800 μg of these particles were used as nuclei (#1). These were dispersed and sonicated for 5 min in 43 μL of EtOH and mixed with 5 μg of pDNA:mCherry:H2B resuspended in 18 μL of nuclease-free dH_2O. Next, 17.3 μL of ammonia and TEOS (2.8 μL) were added to the mixture and the reaction was vortexed for 2 h at room temperature.

2.9. Time-lapse video microscopy

Double-layered DNA@SiO_2 particles (Fig. 5, #2) were resuspended in the culture medium and applied as described in section 2.5. After incubation at 37 °C for 16 h, the medium of each well was replaced with 2 mL of fresh medium. For observation, and to prevent cell overgrowth, cells were split and diluted 1/3 in volume and reseeded in a 6-well plate. After 42 h, the 6-well plate was inserted in a Nikon Ti (Tokyo, Japan) live-station epifluorescence microscope. Cell cultures were recorded for 48 h. All images were pseudo-colored.

3. Results and discussion

3.1. Synthesis and characterization of silica particles loaded with pDNA (DNA@SiO_2)

To prepare DNA@SiO_2 particles, a modified Stöber method was employed based on previous protocols (Experimental Section) [55]. Briefly, purified pDNA was added to the Stöber reaction, facilitating simultaneously nanoparticle formation and nucleic acid encapsulation. We tested three different reaction conditions yielding different sizes of silica (Table S2). Upon refined protocol establishment, we obtained DNA@SiO_2 particles displaying a size of *ca.* 375 nm in diameter, with a ζ-potential of −26.9 ± 3 mV (Fig. 2a–b, Table S3). The *as-prepared* SiO_2 control particles synthesized in parallel, devoid of pDNA, were *ca.* 325 nm and presented a ζ-potential of −24.9 ± 2 mV. This ζ potential increases from −27 mV to -18 mV as soon as the particles are exposed to the culture medium containing serum, when the protein biocorona spontaneously forms, changing their biological identity and being captured by cells in the culture.

To evaluate the encapsulation efficiency of the particles we used an empirical approach. We calculated the encapsulation was in the range of 66 ± 4%, and the approximate average number of plasmids per particle was 20 to 40 molecules of 5000–6000 bp. This represented 0.35% of the total mass of the DNA@SiO_2 particles by TGA (Fig. S1), in agreement with theoretical estimations of *ca.* 5 μg/mg of DNA@SiO_2 particles. The encapsulation efficiency (EE %) and loading capacity (LC %) were additionally calculated by measuring the non-encapsulated pDNA after the Stöber reaction in the supernatant (Fig. S2). The encapsulation efficiency was estimated at 75% and the loading capacity was similar as observed by TG-MS with 0.35%. The seemingly low percentage of the mass of DNA to silica is due to the high density of the encapsulating material compared to other encapsulation systems *e.g.,* lipids.

Finally, the silica encapsulation protocol was tested for different types of pDNA encoding different proteins (Table S1) resulting in virtually identical pDNA@SiO_2 particles (Table S4). The encapsulation of plasmids with various backbones and inserts of different sizes demonstrates the versatility of this system.

3.2. DNA release occurs upon silica dissolution

Based on previous studies demonstrating silica dissolution intracellularly [28,43,44], we now tested the release of the

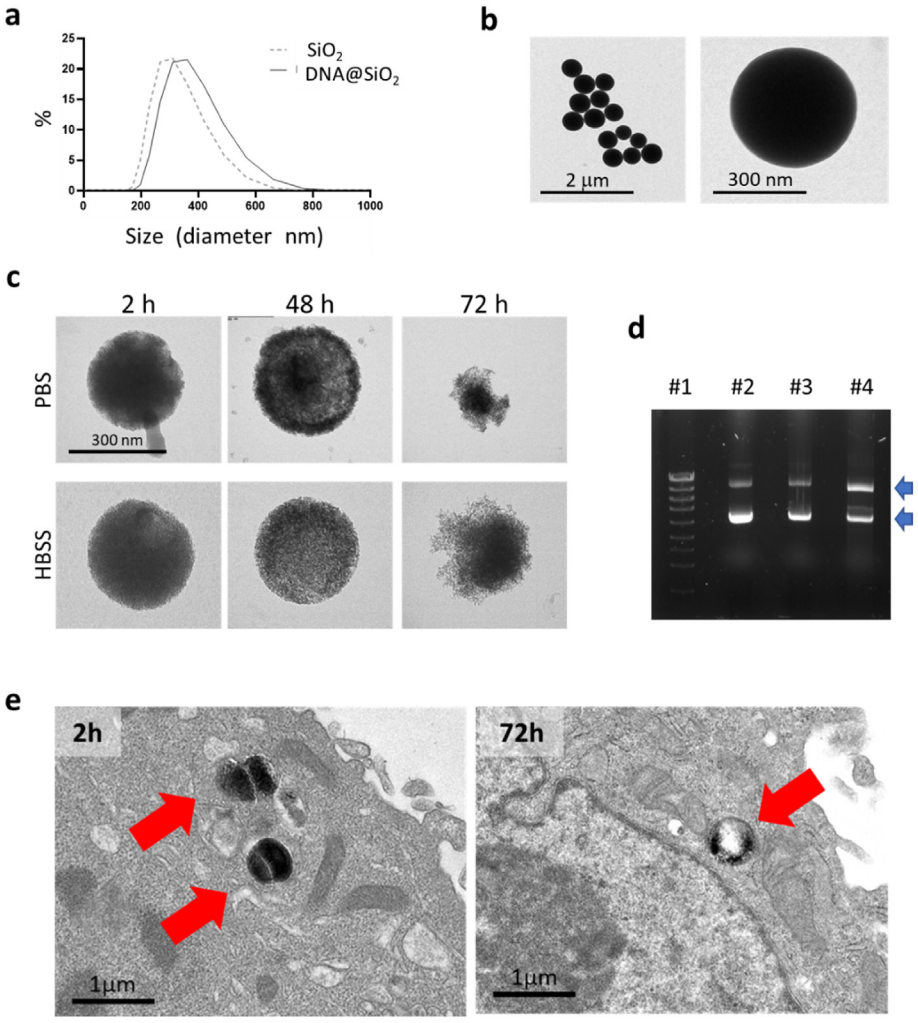

Fig. 2. Synthesis and characterization of silica vectors. a). DLS characterization of DNA@SiO_2 particles. b). TEM images of the pDNA@SiO_2 particles. c). Dissolution of DNA@SiO_2 particles at 37 °C in PBS and HBSS both, physiological buffers d). Agarose gel electrophoresis displaying bands containing the DNA ladder (#1); the *as-prepared* H2B:YFP pDNA (#2); the H2B:YFP extracted pDNA using phosphate buffer (#3) or the NH_4HF etching solution (#4). Blue arrows show the circular and supercoiled pDNA bands. e). *In cellulo* DNA@SiO_2 particle dissolution. TEM images of ultrathin sections of cells treated with DNA@SiO_2. Visible intracellular DNA@SiO_2 particles (red arrows) are intact after cell entry but degraded after 72 h (see Fig. S3). (For interpretation of the references to color in this figure legend, the reader is referred to the Web version of this article.)

encapsulated DNA upon particle dissolution in physiological buffers. For this, we used two physiological saline solutions, phosphate-buffered saline (PBS) (pH 7.4, *ca.* 150 mM NaCl) and cell culture buffered media (pH 7.4, Hank's Balanced Salt Solution, HBSS). Fig. 2c shows TEM images of the degradation of the silica cores of DNA@SiO_2 particles exposed to these physiological buffers at 37 °C for 72 h in both buffers. The apparent faster degradation observed in PBS might be due to the major total concentration of Na^+ and K^+ monovalent counterions in the phosphate salts as previously described [41,56].

The release of pDNA from the dissolving particles was investigated by electrophoresis of the liquid phase on agarose gels. We compared: (i) the *as-produced* pDNA, (ii) the pDNA obtained after silica dissolution in buffers, and (iii) the pDNA extracted from the particles using a hydrofluoric acid treatment [46]. Fig. 2d shows intact released pDNA using both, PBS, and hydrofluoric acid, thus confirming the effective encapsulation/decapsulation of pDNA molecules in amorphous silica particles by direct incorporation of the nucleic acid into the Stöber mixture.

Next, we investigated whether DNA@SiO_2 particles can dissolve intracellularly as described for plain SiO_2 particles [43]. For this, 100 µg/mL of the particles were added to the media of cultured human cells (HEK 293T and HeLa) that were incubated with the particles for different times before fixation, processing for ultramicrotomy, and TEM imaging. Fig. 2e are ultrathin sections of representative cells displaying various intact cytoplasmic DNA@SiO_2 particles (red arrows) 2 h after particle addition of the particles to the culture. As predicted by the *in vitro* studies, intracellular particles were significantly degraded after 72 h. These images suggest that the DNA@SiO_2 particles underwent progressive dissolution in the cellular realm (Fig. S3). In the study, we also evaluated cell viability at different times after exposure to DNA@SiO_2 particles in mammalian cells. The results shown in Fig. S4 indicate that cellular uptake of DNA@SiO_2 particles does not result in a cytotoxic response and that cell viability is not reduced at 48–72 h. These results suggest that silica degradation is biocompatible and validate the use of these particles for biological experiments.

3.3. DNA@SiO_2 particles effectively transfect mammalian cells

After confirmation that silica particles can encapsulate and release nucleic acids, we investigated whether the released pDNA was fully intact and functional. To do this we carried out gene

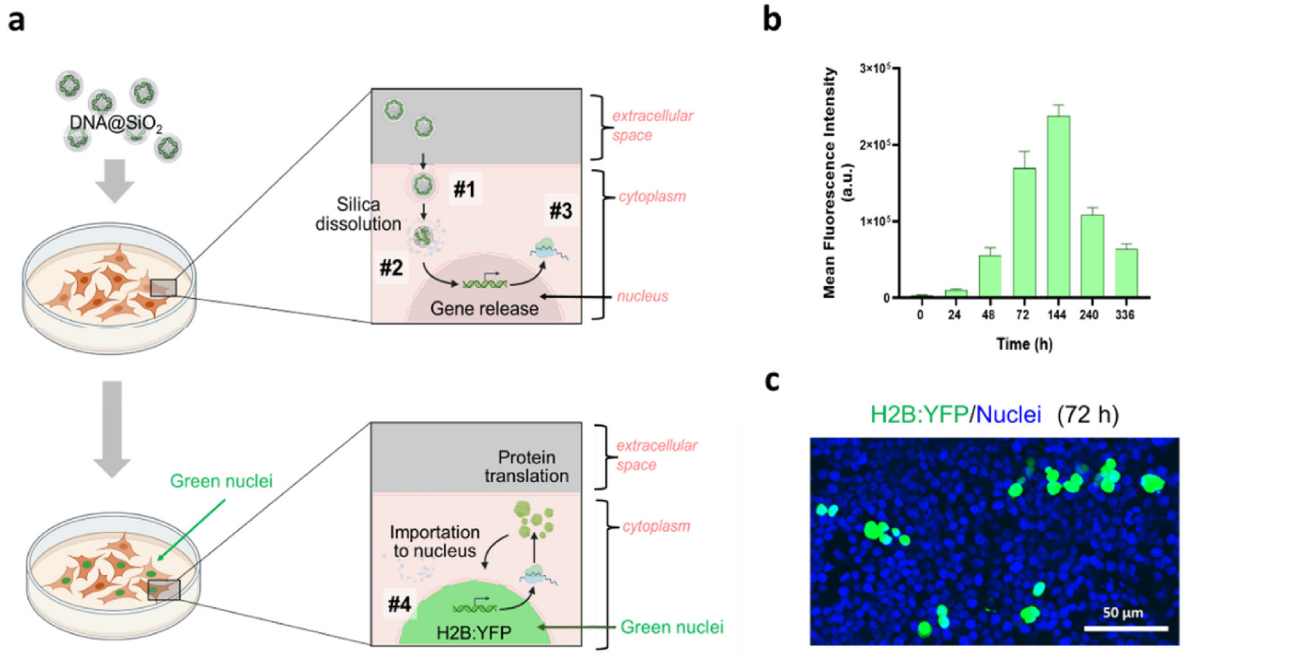

Fig. 3. Transfection experiment. a) Diagram of the DNA@SiO_2 particle intracellular processing. Upon entry, the particle must dissolve in the cytoplasm releasing the DNA (#1) that has to enter the nucleus to be transcribed (#2). In the nucleus, the resulting messenger RNA moves back to the cytoplasm (#3) where the protein is produced by the ribosomes. Upon synthesis, the fluorescent histone protein is immediately imported back into the nucleus (#4) that becomes fluorescent. b) Quantification of H2B:YFP protein expression during 336 h (14 days) after transfection using flow cytometry. Data are shown as the mean ± standard deviation (SD) of 3 experimental replicas (n = 10,000 cells/replica). c) Image of cells treated with DNA@SiO_2 particles expressing fluorescent H2B:YFP 144 h (6 days) post gene transfer.

transfection tests with the DNA@SiO_2 particles. This test should reveal information on whether the encapsulation/release process preserves nucleic acid integrity, as mutations in the plasmid sequence (such as small breaks or chemical modifications) are expected to interfere with gene expression.

As proof of concept, we encapsulated a pDNA encoding the histone H2B that naturally targets the cell nucleus, fused at its carboxyl terminus to the fluorescent protein YFP (H2B:YFP) (Table S3) (Fig. 3). Successful transfection results in a well-defined yellow fluorescence highlighting the nucleus that allows effective quantitative and qualitative assessment of gene expression by flow cytometry or fluorescence microscopy techniques. Fig. 3a shows a diagram of the sequential steps (#1 to #4) required upon DNA@-SiO_2 entry into cells for successful protein expression. The appearance of yellow fluorescence in the nucleus (Fig. 3a, #4) is the way to validate the release of pDNA, and demonstrate the integrity of the nucleic acid.

The expression of pDNA-encoded H2B:YFP protein was assessed at different times for 2 weeks (336 h) after the addition of DNA@-SiO_2 particles to the cell culture. The first fluorescent cells emerged approximately 24 h after treatment, demonstrating that the engineered silica particles were efficient gene delivery devices. From that time point onwards, a progressive increase in nuclear fluorescence was observed. Quantification of H2B:YFP protein expression performed by flow cytometric analysis at different time points revealed that the number of positive cells and the intensity of fluorescence per cell increased gradually over 6 days (144 h after particle exposure) (Fig. 3b and c). To demonstrate the versatility of the encapsulation system and prove that our results were pDNA-dependent, we encapsulated another 5 different pDNA backbones encoding the proteins: HSP70:eGFP, Utrophin-Red, Actin:eGFP, BFP:KDEL, and H2B:mCherry (Table S3). All 5 pDNAs were encapsulated (Table S4), successfully transfecting mammalian cells (Fig. S5). This confirmed that the silica vector can easily be loaded with a variety of different pDNAs bearing several genes with different sizes for cell transfection. These results reinforce the hypothesis that intact, functional pDNA is released from silica particles and provides evidence that these DNA@SiO_2 vectors are suitable as gene delivery devices.

In addition to the transfection efficiency at 72 h of approximately 40% compared to Lipofectamine 2000, the most remarkable feature of this gene transfer system is its extended window of expression of almost one week. This represents a clear advantage over transfection with standard reagents, where gene expression characteristically lasts for an average of 48–72 h (Fig. S6), after which there is a rapid drop in gene expression (*e.g.,* Lipofectamine™ 2000, calcium carbonate, or magnetofection). In all these methods, the release of DNA into the cytoplasm occurs rapidly after entry of the vector into the cell, triggering peak levels of gene expression within a few hours (which may compromise constitutive protein synthesis), and is short-lived, lasting a couple of days [57]. Based on the described particle dissolution process, we believe that the sustained levels of recombinant protein expression observed are dependent on the kinetics of silica dissolution [38]. The protein detection starts to be significant after 48–72 h and agrees with the completed silica degradation observed in TEM imaging after 48 h (Fig. 2e).

3.4. DNA is embedded in the silica matrix

To demonstrate that the pDNA was embedded in the silica colloid (and not adhered to the particle surface as described in previous works), the DNA@SiO_2 particles and naked control pDNA were submerged in a DNase solution (Experimental Section, Fig. S7). After the treatment, we dissolved the particles and extracted the pDNA for examination. Fig. 4 shows how the control *as-prepared* (naked) pDNA (#2) was completely digested upon DNase treatment, but the decapsulated silica-coated pDNA (#4)

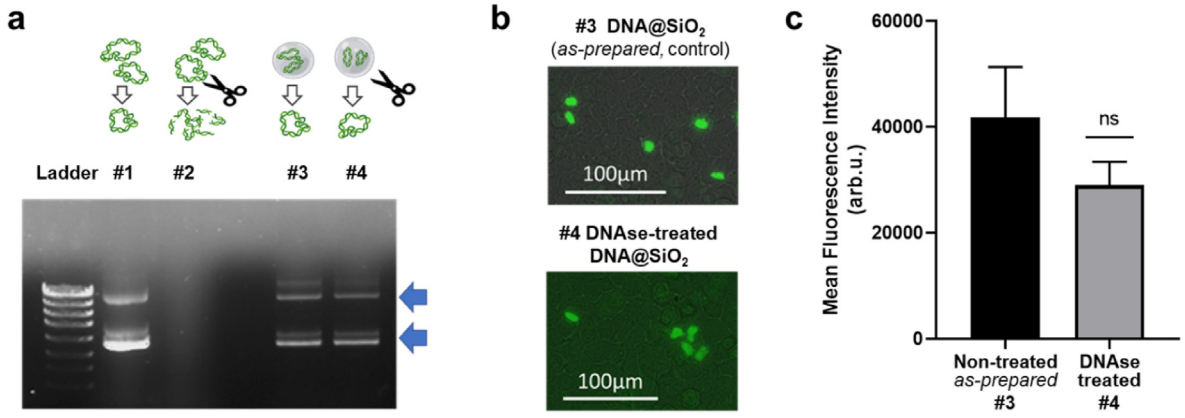

Fig. 4. DNAse treatment of the particles. a) Agarose gel electrophoresis showing (**#1**) Control *as-prepared* (untreated) pDNA; (#2) pDNA treated with DNAse (scissors); (#3) pDNA extracted from the untreated DNA@SiO_2 particles; (#4) pDNA extracted from DNA@SiO_2 particles treated with DNase. Blue arrows show circular and supercoiled DNA bands. b) Fluorescent images of cells transfected with control (#3) or (#4) DNase-treated DNA@SiO_2 particles (72 h after transfection). c) Quantification of H2B:YFP protein expression in cultures exposed to #3 and #4 after 72 h using flow cytometry. Data are shown as the mean ± SD of 3 experimental replicas (n = 10,000 cells/replica, t-test, p = 0.10, ns). A transfection efficiency reduction that is not statistically significant is detected in the DNase-treated particles compared to controls. (For interpretation of the references to color in this figure legend, the reader is referred to the Web version of this article.)

was intact after the nuclease treatment thus, supporting the hypothesis that the DNA was coated and protected inside the silica particles.

The DNase tests were complemented with functional tests that were performed with both, the *as-prepared* and the DNase-treated DNA@SiO_2 particles. Quantification of the cellular protein expression using flow cytometry at 72 h post-transfection revealed a reduction of *ca.* 30% gene expression in cultures exposed to the DNase-treated particles compared to the *as-prepared* DNA@SiO_2 control particles (Fig. 4b and c). This reduction, although not statistically significant, suggests that while most of the DNA is embedded and protected in the particles, some pDNA molecules are susceptible to DNase digestion. We hypothesize that this effect may be inherent to the requirements of the experimental setup as the buffer used during the nuclease test (similar to PBS) likely dissolves the outer layer of silica, partially exposing the DNA and making it accessible to the DNAse. Still, compared to the other silica-based gene transfer vectors, the DNA@SiO_2 particles offer significant protection for the encapsulated DNA from attack by nucleases existing in the biological environments.

3.5. DNA@SiO_2 particles preserve DNA from storage, heat, and ROS

Analogous to insects trapped and preserved in amber, silica is a material that has the potential to function as a protective barrier for molecules encapsulated within it. Hence, to investigate if these DNA@SiO_2 particles as gene delivery devices, improve the stability of the encapsulated nucleic acids, we tested the shelf-life of the vectors in comparison to existing systems.

To explore physical and chemical stresses we first tested the functionality of the system after a prolonged time of storage (1 month) at room temperature (RT) in ethanol (Fig. 5a). TEM imaging revealed that the particles are stable in this condition showing no signs of dissolution (Fig. 5b) and are visually indistinguishable from particles imaged immediately after the synthesis reaction (compare Figs. 1c and 5b). Quantification of gene expression using flow cytometry in cell cultures treated with particles stored for 1 month showed gene expression levels similar to those treated with the *as-prepared* DNA@SiO_2 particles (Fig. 5c). This remarkable stability is extraordinary among the most widely used gene transfer vectors, highlighting that the DNA@SiO_2 particles can easily, and cost-efficiently be stored for a prolonged timeframe not requiring sophisticated or expensive storage conditions.

Next, we investigated the level of protection of the encapsulated DNA against more extreme conditions such as high temperatures (105 °C), ROS (see below), and UV radiation. For these tests, particles were incubated for 45 min at 105 °C, a temperature that would irreversibly denature DNA [58]. To expose the particles to ROS, we used H_2O_2 and Cu^{2+} as described in the supplementary material [48]. Finally, DNA@SiO_2 spheres were irradiated with UVC light (36 W), and used for germicidal purposes, for 60 min (Fig. 5a). In none of the cases were changes in particle morphology observed (Fig. 5b).

After, we tested the functionality of the encapsulated DNA after these treatments by using the treated particles in transfection experiments and quantified the gene expression with flow cytometry assays. The particles were found effective at protecting DNA from heat and ROS exposure with a non-significant reduction in the transfection efficiencies (91%, and 83%, respectively) compared to the *as-prepared* particle controls (Fig. 5c). However, UVC exposure significantly decreased the transfection rate to about 10%. This evidence can be explained by the fact of silica transparency to UV light and the radiation wavelength of 100–280 nm is used to cause DNA damage ultimately rendering the DNA non-functional and impeding transcription [59].

In summary, all these experiments show that silica as a DNA encapsulation vector can significantly improve the stability of nucleic acids used for different purposes for example destined for gene therapy or immunization. The quantitative functional studies suggest that silica spheres can be used to store DNA, protecting it from biological, physical, and chemical attacks, thus permitting long-term storage under standard shelf conditions. Furthermore, these vectors protect the encapsulated DNA under extreme circumstances, including treatments such as denaturing temperatures or ROS, that would damage any most available vectors, whether biological (*e.g.,* virus) or synthetic (*e.g.,* liposomes).

3.6. Layered DNA@SiO_2 particles for sequential gene expression

When a virus infects a mammalian cell, it expresses the viral genes in a sequentially controlled way to manipulate the activity of the host cell (Fig. 6a). Artificially producing gene expression cascades could also have great therapeutic potential, for example, in cumulative disorders (such as neurodegenerative diseases), to first inhibit the expression of a pathological protein, *e.g.,* to produce an interfering RNA, and then activate repair mechanisms.

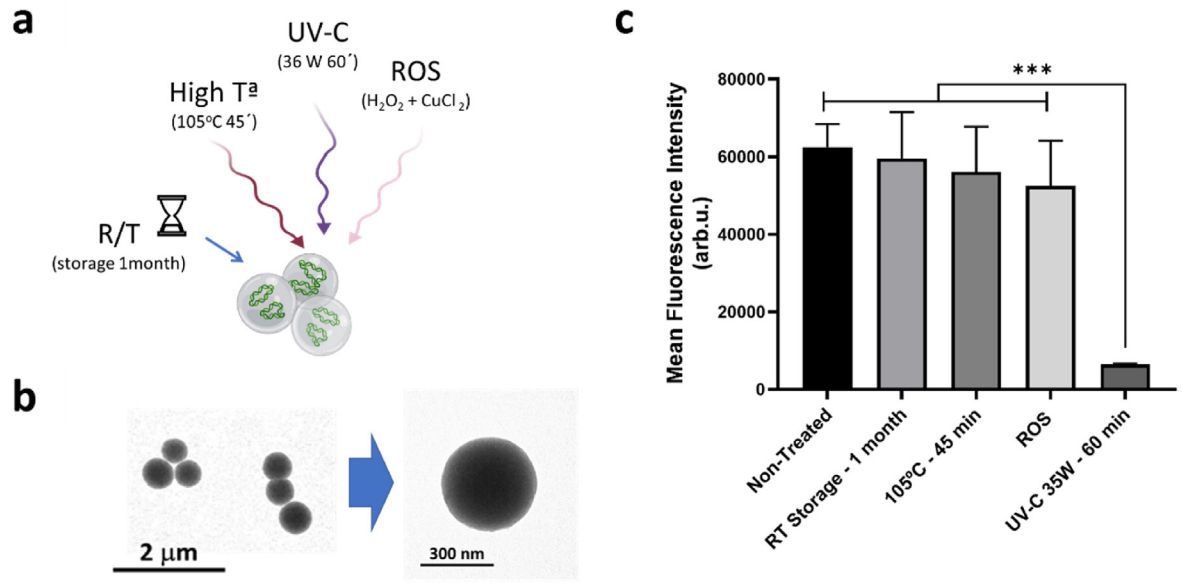

Fig. 5. DNA@SiO_2 particle stability. a) Diagram of the experimental procedure. TEM images of the DNA@SiO_2 particles after 1-month room-temperature (RT) storage in a transparent vial. b) Diagram of the experimental procedure. c) Quantification using flow cytometry of H2B:YFP protein expression in cultures after 72 h being exposed to the particles stored for 1 month at RT and treated with high temperature, ROS, or UVC. A non-significant reduction in the transfection efficiency in the stored particles is observed. On the contrary, a significant reduction in the transfection efficiency is observed for particles treated with UVC. Flow cytometry quantitative data (Fig. S8) are shown as the mean ± SD of 3 experimental replicas (n = 10,000 cells/replica, t-test, ***p = 0.0001 ANOVA).

Current gene delivery systems do not allow the sequential expression of genes. This can neither be achieved by combining several vectors carrying different genes nor by encapsulating several genes simultaneously in one vector. So, we investigated whether we could modify our design to trigger the expression of different genes in a chronologically controlled way as viruses do. To do this, we produce silica particles to encapsulate different pDNAs in concentric layers of silica that we hypothesize will progressively release the different pDNAs, triggering the sequential expression of the proteins encoded in them.

As a proof-of-concept experiment and, to unambiguously identify sequentially expressed proteins, we used genes encoding two distinctive fluorescent proteins. Thus, we chose one gene encoding the nuclear histone H2B fused to the red fluorescent protein mCherry (H2B:mCherry), and a second gene, expected to be released and expressed later, encoding the cytoplasmic heat shock protein 70 fused to GFP (Hsp70:GFP) (Fig. 6b, Table S3).

To prepare a double pDNA vector, Hsp70:GFP pDNA particles of *ca.* 200 nm diameter were prepared as described (Fig. 6c-d, #1) (Experimental section 2.9). The next silica layer containing H2B:mCherry pDNA was produced using these Hsp70:GFP@SiO_2 particles as seeds. The Stöber conditions for the second silica layer were similar. Briefly,. 800 µg of the Hsp70:GFP@SiO_2 silica particles were mixed with the outer layer pDNA (*e.g.,* mCherry:H2B) and resuspended in water/EtOH before ammonia and TEOS were added. The HSP70:GFP@SiO_2@H2B:mCherry@SiO_2 double-layered particles, with an approximate size of *ca.* 500 nm diameter, were obtained after *ca.* 2 h vortex at room temperature (Table S2). The same strategy was used to synthesize triple-layered particles that finally had a size of *ca.* 700 nm by DLS. Unfortunately, as demonstrated for other systems [51], these larger double/triple-layered particles were less efficient in gene transduction (Fig. 6f).

The double-layered systems were transfected and *time-lapse* video-imaged to verify the sequential expression sequence (Fig. 6e–g, S8). Based on the DNA@SiO_2 particle dissolution model discussed (from the outside in), the H2B:mCherry coding plasmid was programmed to be released and expressed before the Hsp70:GFP plasmid. This will make the red fluorescence of H2B:mCherry visible in the cellular nuclei, before the green fluorescence of Hsp70:GFP appears in the cellular cytoplasm. Fig. 6e shows some representative sequential frames from Video S1 demonstrating how these effectively transfected cells follow the designed gene expression program, expressing first the red fluorescent nuclear protein and, approximately 10 h later, the green fluorescent protein. Quantification of fluorescent protein expression at 24, 48, and 72 h after particle treatment confirmed that most cells (*ca.* 80%, as determined by spectral flow cytometric analysis) were expressing the nuclear red fluorescent protein (red, Fig. 6g). At 72 h, co-expression of both genes was visible in about half of the transfected cells. At that time, approximately 20% of the cells had only detectable green fluorescence, suggesting that nuclear protein expression might have been downregulated after several post-transfection cell division cycles.

Supplementary data related to this article can be found at https://doi.org/10.1016/j.mtadv.2023.100357.

Finally, to demonstrate the versatility of the layered particle technology, combinations of plasmids encoding different fluorescent proteins were used to produce three-layered particles (Table S3, Experimental Section). These particles were tested by performing transfection and demonstrating how they also activated the sequential expression of programmed multicolor proteins. (Figs. S10, S11, S12).

4. Discussion

Here we developed a novel gene delivery carrier system using amorphous silica as the encapsulating material. The silica nanoparticles effectively functioned as a biological barrier protecting the encapsulated DNA from digestion by environmental nucleases, against physical (heat) and chemical (ROS) stresses, and were able

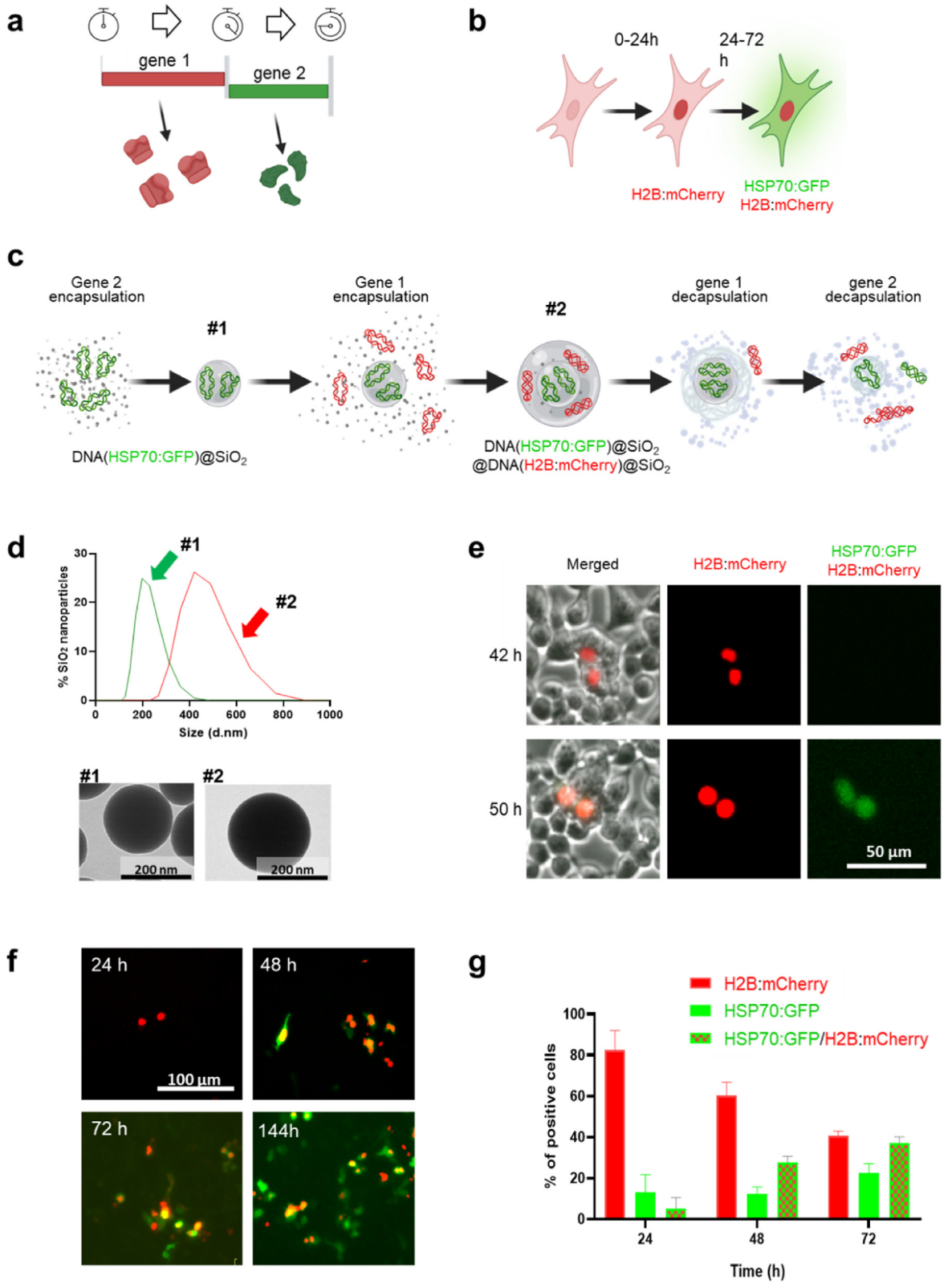

Fig. 6. Design of SiO_2 vectors for sequential gene expression. a) Diagram of the programmed gene expression and b) expected time sequence/localization of the fluorescent proteins in the transfected cells. c) Diagram of the particle synthesis design and DNA sequential encapsulation-decapsulation steps. d) DLS and TEM characterization of the core (#1) and the final bilayer particles (#2) containing HSP70:GFP and H2B:mCherry pDNAs. e) Representative photograms of a live-cell fluorescent microscopy Video S1 demonstrating two cells expressing sequentially the red and green fluorescent proteins, as programmed. f) Representative images of cultures of cells treated with the HSP70:GFP@SiO_2@H2B:mCherry@SiO_2 particles. g) Quantification by flow cytometry of fluorescent protein expression at 24, 48, and 72 h. Approximately 10,000 cells were analyzed per experimental replica ($n = 3$) (Fig. S9). Data are shown as the mean ± SD. (For interpretation of the references to color in this figure legend, the reader is referred to the Web version of this article.)

to deliver functional cargo to cells. Combined, these are excellent protective properties enabling cost-efficient storage as it doesn't require cost intense storage conditions.

Another novel characteristic of the DNA@SiO_2 particles is the significantly extended duration of transfected gene expression compared to existing devices, which could prove advantageous for several applications in nanomedicine when used for gene therapy or immunization purposes among many others. Furthermore, this extraordinary gene delivery system also allows programming the sequential expression of various proteins by synthesizing layered particles encapsulating different pDNAs. Because the release of the pDNAs is linked to the relatively slow dissolution process of the particles, genes get expressed with a time delay in the reverse order of particle synthesis (Fig. 5c).

Hence, this novel method enables entirely new possibilities in gene expression manipulation. For example, it may allow the treatment of neurodegenerative diseases where toxic proteins accumulate irreversibly [60,61]. In these diseases, sequential gene expression could first be used to block the expression of defective genes, and then trigger the production of either repair proteins or healthy proteins. But there are many other interesting potential applications in the field of biotechnology and medicine. These particles could be used to modify gene expression in living organisms in a precise and controlled manner, for example by injection into the diseased tissue, or using targeting ligands, thus opening a wide range of possibilities for treatments and cures of genetic disorders by selective activation of gene expression in the affected cells [62].

Another possible application is the treatment of cancer to control the expression of genes involved in cell growth, division, and death. In a targeted way, these particles could be used against cancer [63]. Additionally, by triggering the expression of genes involved in immune response, these particles can also enhance the body's natural ability to fight infectious diseases or cancer [64]. But these nanoparticles can also be used in regenerative medicine to stimulate the growth of new tissues to enhance the expression of genes involved in cell growth and differentiation, to promote the regeneration of damaged tissues, leading to better healing and reduced scarring [65]. Also, these applications in the clinical world could be widely extended to other fields, for example, agricultural biotechnology. These particles could be used to activate the expression of genes that improve growth and stress tolerance, making crops more productive and resistant to environmental challenges, resulting in higher yields and greater food security, ultimately improving crop yields or resistance to pests and diseases [47].

Thanks to the straightforward modification of the nanoparticle synthesis reaction, this system allows the encapsulation of a wide range of plasmids plasmid backbones of different sizes bearing different genes, while maintaining their functionality in a very cost-effective way, increasing their versatility and attractiveness for a wide range of potential applications. It also has the potential to be easily scalable for industrial production and clinical evaluation. Besides, the surface of these particles is highly customizable and can be easily functionalized to target, for example, to introduce genes into cells with certain receptors or to cross the blood-brain barrier. Together, these properties make this new vector a viral-mimetic system, which could find application in many different aspects of nanomedicine.

5. Conclusions

In summary, these devices satisfy criteria such as (i) being cost-efficient, (ii) reproducible, (iii) can be produced and tested industrially, (iv) displaying excellent storability, (v) can be efficiently functionalized to achieve fully customizable, cell-targeted systems, and (vi) have no DNA type/size limitations, etc. Other great added values of these vectors are: (i) they protect DNA (from nuclease attack, high temperature, ROS degradation); (ii) do not produce cytotoxicity; (iii) significantly extends the length of the window of transduced gene expression by several days; and finally (iv) the system makes possible to control the expression of different genes in a sequential and chronologically programmable manner, a unique feature among vectors in current use. All these properties make this new gene transfer system a robust and efficient vector that will surely allow, in the medium and long term, the development of gene therapies, immunization systems, or personalized medicines that can be scalable at an industrial level and that, with few logistical drawbacks, allow the analysis of large batches and long-distance distribution.

Credit author statement

ML Fanarraga, as corresponding author is responsible for ensuring that the descriptions are accurate and agreed by all authors.Conceptualization: MLF. MAC, Methodology: ARV, LMA, LGH, MAC, MLF, Validation ARV, LMA, LGH, Formal analysis ARV, LMA, LGH, MLF, Investigation ARV, MLF, Resources MLF, Data Curation, ARV, LMA, LGH, MLF, Writing - Original Draft ARV, MLF, Writing - Review & Editing ARV, LGH, MLF, Supervision, MLF, Project administration MAC, MLF, Funding acquisition MAC, MLF

Declaration of competing interest

The authors declare that they have no known competing financial interests or personal relationships that could have appeared to influence the work reported in this paper.

Data availability

Data will be made available on request.

Acknowledgments

We are grateful to D. Muñoz for her technical support and Dr. Kirst for his criticisms of the manuscript. MLF acknowledges the financial support from the Spanish Instituto de Salud Carlos iii, and the European Union FEDER funds under Projects ref. PI22/00030 and PI19/00349, co-funded by the European Regional Development Fund, “Investing in your future” and Grant TED2021-129248 B−I00 funded by MCIN/AEI/10.13039/501100011033 and by the “European Union Next Generation EU/PRTR”. We also thank the Gobierno Regional de Cantabria and IDIVAL for the project Refs IDI 20/22, INNVAL21/19, and IDI-020-022 fellowship to ARV and technological and administrative services. MACD acknowledges financial support from the Spanish Ministerio de Economía y Competitividad under grant PID2020-113704RB-I00, Xunta de Galicia/FEDER (IN607A 2018/5 and Centro Singular de Investigación de Galicia, Acc. 2019−2022, ED431G 2019−06), 0712/ACUINANO1E, 0624/2IQBIONEURO6E cofounded by FEDER through the program Interreg V-A Espana-Portugal (POCTEP), and NANOCULTURE (ERDF: 1.102.531) Interreg Atlantic Area, the European Union (European Regional Development Fund-ERDF). LMC acknowledges the Margarita Salas requalification grants for the training of young doctors Ref.: REC-Salas21, Uvigo-UC (Ministerio de Universidades). Figures and graphs have been created with BioRender software (BioRender.com, License ID: 9519A1C8-0002). We are grateful to Dr. Lansford, Dr. Parton, Dr. Greene, Dr. Davidson, Dr. Bement and Dr. Voeltz for the plasmids references in Table S1 (obtained fron Addgene).

Appendix A. Supplementary data

Supplementary data to this article can be found online at https://doi.org/10.1016/j.mtadv.2023.100357.

References

[1] K.A. High, M.G. Roncarolo, Gene therapy, Scientist 10 (1996) 455–464, https://doi.org/10.1056/NEJMra1706910.

[2] FDA, Approval Brings First Gene Therapy to the United States, FDA U.S. Food Drug, 2017.

[3] S. Mavrikou, G. Moschopoulou, A. Zafeirakis, K. Kalogeropoulou, G. Giannakos, A. Skevis, S. Kintzios, An ultra-rapid biosensory point-of-care (POC) assay for prostate-specific antigen (PSA) detection in human serum, Sensors 18 (2018) 3834, https://doi.org/10.3390/S18113834.

[4] C.E. Dunbar, K.A. High, J.K. Joung, D.B. Kohn, K. Ozawa, M. Sadelain, Gene therapy comes of age, Science 80 (2018) 359, https://doi.org/10.1126/science.aan4672.

[5] S.L. Ginn, A.K. Amaya, I.E. Alexander, M. Edelstein, M.R. Abedi, Gene therapy clinical trials worldwide to 2017: an update, J. Gene Med. 20 (2021), e3015, https://doi.org/10.1002/JGM.3015.

[6] C. Raoul, T. Abbas-Terki, J.-C. Bensadoun, S. Guillot, G. Haase, J. Szulc, C.E. Henderson, P. Aebischer, Lentiviral-mediated silencing of SOD1 through RNA interference retards disease onset and progression in a mouse model of ALS, Nat. Med. 11 (2005) 423–428, https://doi.org/10.1038/nm1207.

[7] A. Ganju, S. Khan, B.B. Hafeez, S.W. Behrman, M.M. Yallapu, S.C. Chauhan, M. Jaggi, miRNA nanotherapeutics for cancer, Drug Discov. Today 22 (2017) 424–432, https://doi.org/10.1016/j.drudis.2016.10.014.

[8] S. Ghosh, A.M. Brown, C. Jenkins, K. Campbell, Viral vector systems for gene therapy: a comprehensive literature review of progress and biosafety challenges, Appl. Biosaf. 25 (2020) 7–18, https://doi.org/10.1177/1535676019899502.

[9] I. Lostalé-Seijo, J. Montenegro, Synthetic materials at the forefront of gene delivery, Nat. Rev. Chem 2 (2018) 258–277, https://doi.org/10.1038/s41570-018-0039-1.

[10] D. Guimarães, A. Cavaco-Paulo, E. Nogueira, Design of liposomes as drug delivery system for therapeutic applications, Int. J. Pharm. 601 (2021), 120571, https://doi.org/10.1016/J.IJPHARM.2021.120571.

[11] J. Buck, P. Grossen, P.R. Cullis, J. Huwyler, D. Witzigmann, Lipid-based DNA therapeutics: hallmarks of non-viral gene delivery, ACS Nano 13 (2019) 3754–3782, https://doi.org/10.1021/acsnano.8b07858.

[12] L. Duan, Y. Yan, J. Liu, B. Wang, P. Li, Q. Hu, W. Chen, Target delivery of small interfering RNAs with vitamin E-coupled nanoparticles for treating hepatitis C, Sci. Rep. 6 (2016), 24867, https://doi.org/10.1038/srep24867.

[13] C. Uherek, W. Wels, DNA-carrier proteins for targeted gene delivery, Adv. Drug Deliv. Rev. 44 (2000) 153–166, https://doi.org/10.1016/S0169-409X(00)00092-2.

[14] H. Zare, S. Ahmadi, A. Ghasemi, M. Ghanbari, N. Rabiee, M. Bagherzadeh, M. Karimi, T.J. Webster, M.R. Hamblin, E. Mostafavi, Carbon nanotubes: smart drug/gene delivery carriers, Int. J. Nanomed. 16 (2021) 1681, https://doi.org/10.2147/IJN.S299448.

[15] S. Taghavi, K. Abnous, S.M. Taghdisi, M. Ramezani, M. Alibolandi, Hybrid carbon-based materials for gene delivery in cancer therapy, J. Contr. Release 318 (2020) 158–175, https://doi.org/10.1016/j.jconrel.2019.12.030.

[16] S. Maleki Dizaj, M. Barzegar-Jalali, M. Hossein Zarrintan, K. Adibkia, F. Lotfipour, Calcium carbonate nanoparticles as cancer drug delivery system, Expet Opin. Drug Deliv. 12 (2015) 1649–1660, https://doi.org/10.1517/17425247.2015.1049530.

[17] H. Li, S. Zha, H. Li, H. Liu, K.L. Wong, A.H. All, Polymeric dendrimers as nanocarrier vectors for neurotheranostics, Small 18 (2022), 2203629, https://doi.org/10.1002/SMLL.202203629.

[18] S.C. De Smedt, J. Demeester, W.E. Hennink, Cationic polymer based gene delivery systems, Pharm. Res. (N. Y.) 17 (2000) 113–126, https://doi.org/10.1023/A:1007548826495.

[19] M. Zheng, W. Tao, Y. Zou, O.C. Farokhzad, B. Shi, Nanotechnology-based strategies for siRNA brain delivery for disease therapy, Trends Biotechnol. 36 (2018) 562–575, https://doi.org/10.1016/J.TIBTECH.2018.01.006.

[20] W.B. Liechty, R.L. Scheuerle, J.E. Vela Ramirez, N.A. Peppas, Cytoplasmic delivery of functional siRNA using pH-Responsive nanoscale hydrogels, Int. J. Pharm. 562 (2019) 249–257, https://doi.org/10.1016/j.ijpharm.2019.03.013.

[21] H.F. Teixeira, F. Bruxel, M. Fraga, R.S. Schuh, G.K. Zorzi, U. Matte, E. Fattal, Cationic nanoemulsions as nucleic acids delivery systems, Int. J. Pharm. 534 (2017) 356–367, https://doi.org/10.1016/j.ijpharm.2017.10.030.

[22] A. Mahmood, F. Prüfert, N.A. Efiana, M.I. Ashraf, M. Hermann, S. Hussain, A. Bernkop-Schnürch, Cell-penetrating self-nanoemulsifying drug delivery systems (SNEDDS) for oral gene delivery, Expet Opin. Drug Deliv. 13 (2016) 1503–1512, https://doi.org/10.1080/17425247.2016.1213236.

[23] J. Panyam, V. Labhasetwar, Biodegradable nanoparticles for drug and gene delivery to cells and tissue, Adv. Drug Deliv. Rev. 64 (2012) 61–71, https://doi.org/10.1016/j.addr.2012.09.023.

[24] S. Nagachinta, B.L. Bouzo, A.J. Vazquez-Rios, R. Lopez, M. de la Fuente, Sphingomyelin-based nanosystems (SNs) for the development of anticancer miRNA therapeutics, Pharmaceutics 12 (2020) 189, https://doi.org/10.3390/pharmaceutics12020189.

[25] S.J. Doxsey, J. Sambrook, A. Helenius, J. White, An efficient method for introducing macromolecules into living cells, J. Cell Biol. 101 (1985) 19–27, https://doi.org/10.1083/jcb.101.1.19.

[26] European Medicines Agency Committee for Advanced Therapies (CAT), Guideline on the quality, non-clinical and clinical aspects of gene therapy medicinal products, Eur. Med. Agency Guidel. 44 (2018) 1–41.

[27] A.M. Carvalho, R.A. Cordeiro, H. Faneca, Silica-based gene delivery systems: from design to therapeutic applications, Pharmaceutics 12 (2020) 1–45, https://doi.org/10.3390/pharmaceutics12070649.

[28] J.G. Croissant, K.S. Butler, J.I. Zink, C.J. Brinker, Synthetic amorphous silica nanoparticles: toxicity, biomedical and environmental implications, Nat. Rev. Mater. 5 (2020) 886–909, https://doi.org/10.1038/s41578-020-0230-0.

[29] S. Cox, A. Sandall, L. Smith, M. Rossi, K. Whelan, Food additive emulsifiers: a review of their role in foods, legislation and classifications, presence in food supply, dietary exposure, and safety assessment, Nutr. Rev. 79 (2021) 726–741, https://doi.org/10.1093/NUTRIT/NUAA038.

[30] Z. Li, J.C. Barnes, A. Bosoy, J.F. Stoddart, J.I. Zink, Mesoporous silica nanoparticles in biomedical applications, Chem. Soc. Rev. 41 (2012) 2590–2605, https://doi.org/10.1039/c1cs15246g.

[31] J.L. Paris, M. Vallet-Regí, Mesoporous silica nanoparticles for co-delivery of drugs and nucleic acids in oncology: a review, Pharmaceutics 12 (2020) 1–21, https://doi.org/10.3390/pharmaceutics12060526.

[32] X. Huang, L. Li, T. Liu, N. Hao, H. Liu, D. Chen, F. Tang, The shape effect of mesoporous silica nanoparticles on biodistribution, clearance, and biocompatibility in vivo, ACS Nano 5 (2011) 5390–5399, https://doi.org/10.1021/nn200365a.

[33] J. Lu, M. Liong, Z. Li, J.I. Zink, F. Tamanoi, Efficiency of mesoporous silica nanoparticles for cancer therapy in animals, Small 6 (2010) 1794–1805, https://doi.org/10.1002/smll.201000538.

[34] J.A. Bonventre, J.B. Pryor, B.J. Harper, S.L. Harper, The impact of aminated surface ligands and silica shells on the stability, uptake, and toxicity of engineered silver nanoparticles, J. Nanoparticle Res. 16 (2014) 2761, https://doi.org/10.1007/s11051-014-2761-z.

[35] E. Navarro-Palomares, P. González-Saiz, C. Renero-Lecuna, R. Martín Rodríguez, F. Aguado, D. González-Alonso, L. Fernandez Barquin, J.A. Gonzalez, M. Bañobre-López, M.L. Fanarraga, R. Valiente, R. Martín-Rodríguez, F. Aguado, D. González-Alonso, L. Fernández Barquín, J. González, M. Bañobre-López, M.L.M.L. Fanarraga, R. Valiente, Dye-doped biodegradable nanoparticle SiO2 coating in zinc- and iron-oxide nanoparticles to improve biocompatibility and in vivo imaging studies, Nanoscale 12 (2020) 6164–6175, https://doi.org/10.1039/c9nr08743e.

[36] H.L. Ding, Y.X. Zhang, S. Wang, J.M. Xu, S.C. Xu, G.H. Li, Fe3O4@SiO2 core/shell nanoparticles: the silica coating regulations with a single core for different core sizes and shell thicknesses, Chem. Mater. 24 (2012) 4572–4580, https://doi.org/10.1021/cm302828d.

[37] R.N.M. Carmen Vogt, Muhammet S. Toprak, Mamoun Muhammed, Sophie Laurent, Jean-Luc Bridot, High quality and tuneable silica shell-magnetic core nanoparticles, J. Nanoparticle Res. 12 (2010) 1137–1147, https://doi.org/10.1007/s11051-009-9661-7.

[38] J.G. Croissant, Y. Fatieiev, N.M. Khashab, Degradability and clearance of silicon, organosilica, silsesquioxane, silica mixed oxide, and mesoporous silica nanoparticles, Adv. Mater. 29 (2017), 1604634, https://doi.org/10.1002/adma.201604634.

[39] J.G. Croissant, Y. Fatieiev, A. Almalik, N.M. Khashab, Mesoporous silica and organosilica nanoparticles : physical chemistry , biosafety , delivery strategies , and biomedical applications, Adv. Healthc. Mater. 7 (2017), 1700831, https://doi.org/10.1002/adhm.201700831.

[40] K.S. Finnie, D.J. Waller, F.L. Perret, A.M. Krause-Heuer, H.Q. Lin, J.V. Hanna, C.J. Barbé, Biodegradability of sol-gel silica microparticles for drug delivery, J. Sol. Gel Sci. Technol. 49 (2009) 12–18, https://doi.org/10.1007/s10971-008-1847-4.

[41] P.M. Dove, N. Han, A.F. Wallace, J.J. De Yoreo, Kinetics of amorphous silica dissolution and the paradox of the silica polymorphs, Proc. Natl. Acad. Sci. U.S.A. 105 (2008) 9903–9908, https://doi.org/10.1073/pnas.0803798105.

[42] Y. Shi, C. Hélary, B. Haye, T. Coradin, C. Helary, B. Haye, T. Coradin, C. Hélary, B. Haye, T. Coradin, extracellular versus intracellular degradation of nanostructured silica particles, Langmuir 34 (2018) 406–415, https://doi.org/10.1021/acs.langmuir.7b03980. Extracellular versus Intracellular Degradation of Nanostructured Silica ParticlesShi.

[43] N. Iturrioz-Rodríguez, M.A. Correa-Duarte, R. Valiente, M.L. Fanarraga, Engineering sub-cellular targeting strategies to enhance safe cytosolic silica particle dissolution in cells, Pharmaceutics 12 (2020) 487, https://doi.org/10.3390/pharmaceutics12060487.

[44] J.L. Paris, M. Colilla, I. Izquierdo-Barba, M. Manzano, M. Vallet-Regí, Tuning mesoporous silica dissolution in physiological environments: a review, J. Mater. Sci. 52 (2017) 8761–8771, https://doi.org/10.1007/s10853-017-0787-1.

[45] G. Mikutis, C.A. Deuber, L. Schmid, A. Kittilä, N. Lobsiger, M. Puddu, D.O. Asgeirsson, R.N. Grass, M.O. Saar, W.J. Stark, Silica-encapsulated DNA-based tracers for aquifer characterization, Environ. Sci. Technol. 52 (2018) 12142–12152, https://doi.org/10.1021/acs.est.8b03285.

[46] D. Kapusuz, C. Durucan, Exploring encapsulation mechanism of DNA and mononucleotides in sol-gel derived silica, J. Biomater. Appl. 32 (2017) 114–125, https://doi.org/10.1177/0885328217713104.

[47] O.I.S. Torney, B.G. Trewyn, V.S. Lin, K.A.N. Wang, Mesoporous silica nanoparticles deliver DNA and chemicals into plants, Nat. Nanotechnol. 2 (2007) 295–300, https://doi.org/10.1038/nnano.2007.108.
[48] D. Paunescu, M. Puddu, J.O.B. Soellner, P.R. Stoessel, R.N. Grass, Reversible DNA encapsulation in silica to produce ROS-resistant and heat-resistant synthetic DNA "fossils, Nat. Protoc. 8 (2013) 2440–2448, https://doi.org/10.1038/nprot.2013.154.
[49] D.J. Bharali, I. Klejbor, E.K. Stachowiak, P. Dutta, I. Roy, N. Kaur, E.J. Bergey, P.N. Prasad, M.K. Stachowiak, T.Y. Ohulchanskyy, D.J. Bharali, H.E. Pudavar, R.A. Mistretta, N. Kaur, P.N. Prasad, I. Klejbor, E.K. Stachowiak, P. Dutta, I. Roy, N. Kaur, E.J. Bergey, P.N. Prasad, M.K. Stachowiak, Organically modified silica nanoparticles: a nonviral vector for in vivo gene delivery and expression in the brain, Proc. Natl. Acad. Sci. U.S.A. 102 (2005) 11539–11544, https://doi.org/10.1073/pnas.0504926102.
[50] W. Cha, R. Fan, Y. Miao, Y. Zhou, C. Qin, X. Shan, X. Wan, J. Li, Mesoporous silica nanoparticles as carriers for intracellular delivery of nucleic acids and subsequent therapeutic applications, Molecules 22 (2017) 782, https://doi.org/10.3390/molecules22050782.
[51] M. Yu, Y. Niu, J. Zhang, H. Zhang, Y. Yang, E. Taran, S. Jambhrunkar, W. Gu, P. Thorn, C. Yu, Size-dependent gene delivery of amine-modified silica nanoparticles, Nano Res. 9 (2016) 291–305, https://doi.org/10.1007/s12274-015-0909-5.
[52] H. Zarei, R. Kazemi Oskuee, M.Y. Hanafi-Bojd, L. Gholami, L. Ansari, B. Malaekeh-Nikouei, Enhanced gene delivery by polyethyleneimine coated mesoporous silica nanoparticles 24 (2018) 127–132, https://doi.org/10.1080/10837450.2018.1431930.
[53] W. Stöber, A. Fink, E. Bohn, Controlled growth of monodisperse silica spheres in the micron size range, J. Colloid Interface Sci. 26 (1968) 62–69, https://doi.org/10.1016/0021-9797(68)90272-5.
[54] O.I. Aruoma, B. Halliwell, E. Gajewski, M. Dizdaroglu, Copper-ion-dependent damage to the bases in DNA in the presence of hydrogen peroxide, Biochem. J. 273 (1991) 601–604, https://doi.org/10.1042/bj2730601.
[55] W. Stöber, A. Fink, E.E. Bohn, W. Stöber, A. Fink, E.E. Bohn, Controlled growth of monodisperse silica spheres in the micron size range, Colloid Interface Sci. 26 (1998) 27, https://doi.org/10.1016/0021-9797(68)90272-5.
[56] J.P. Icenhower, P.M. Dove, The dissolution kinetics of amorphous silica into sodium chloride solutions: effects of temperature and ionic strength, Geochem. Cosmochim. Acta 64 (2000) 4193–4203, https://doi.org/10.1016/S0016-7037(00)00487-7.
[57] H.S. Liu, M.S. Jan, C.K. Chou, P.H. Chen, N.J. Ke, Is green fluorescent protein toxic to the living cells? Biochem. Biophys. Res. Commun. 260 (1999) 712–717, https://doi.org/10.1006/BBRC.1999.0954.
[58] R.M. Wartell, A.S. Benight, Thermal denaturation of DNA molecules: a comparison of theory with experiment, Phys. Rep. 126 (1985) 67–107, https://doi.org/10.1016/0370-1573(85)90060-2.
[59] R.P. Sinha, D.P. Häder, UV-induced DNA damage and repair: a review, Photochem. Photobiol. Sci. 1 (2002) 225–236, https://doi.org/10.1039/B201230H.
[60] M. Donnelley, D. Parsons, I. Prichard, Perceptions of airway gene therapy for cystic fibrosis, Expet Opin. Biol. Ther. 23 (2022) 103–113, https://doi.org/10.1080/14712598.2022.2150544.
[61] A. Monaco, A. Fraldi, Protein aggregation and dysfunction of autophagy-lysosomal pathway: a vicious cycle in lysosomal storage diseases, Front. Mol. Neurosci. 13 (2020) 37, https://doi.org/10.3389/FNMOL.2020.00037/BIBTEX.
[62] A. Shahryari, M.S. Jazi, S. Mohammadi, H.R. Nikoo, Z. Nazari, E.S. Hosseini, I. Burtscher, S.J. Mowla, H. Lickert, Development and clinical translation of approved gene therapy products for genetic disorders, Front. Genet. 10 (2019) 868, https://doi.org/10.3389/FGENE.2019.00868/BIBTEX.
[63] Q. Yang, Y. Zhou, J. Chen, N. Huang, Z. Wang, Y. Cheng, Gene therapy for drug-resistant glioblastoma via lipid-polymer hybrid nanoparticles combined with focused ultrasound, Int. J. Nanomed. 16 (2021) 185–199, https://doi.org/10.2147/IJN.S286221.
[64] J. Nam, S. Son, K.S. Park, W. Zou, L.D. Shea, J.J. Moon, Cancer nanomedicine for combination cancer immunotherapy, Nat. Rev. Mater. 4 (2019) 398–414, https://doi.org/10.1038/s41578-019-0108-1.
[65] J.K. Venkatesan, A. Rey-Rico, M. Cucchiarini, Current trends in viral gene therapy for human orthopaedic regenerative medicine, Tissue Eng. Regen. Med. 16 (2019) 345–355, https://doi.org/10.1007/S13770-019-00179-X.